Volume 1 - Issue 1
SVR-Materials Science and Engineering Technology
Research Article
SVR PUBLISHERS
OPEN ACCESS

Effect of the deposition strategy on Al-Cu alloy wire + arc additive manufacture

Kwasi Frimpong Ayarkwa[ab]*, Zsolt Pinter[a], Eloise Eimer[a], Stewart Williams[a], Jialuo Ding[a], Wojciech Suder[a]

[a] Welding Engineering and Laser Processing Centre, Cranfield University, Bedfordshire, MK43 0AL, UK

[b] The Manufacturing Technology Centre, Pilot Way, Ansty Park, Coventry, CV79JU

*Corresponding author: Kwasi Frimpong Ayarkwa, Welding Engineering and Laser Processing Centre, Cranfield University, Bedfordshire, MK430AL, UK.

Received: April 09, 2021 **Published:** April 28, 2021

Abstract

The effect of the deposition strategy on wire + arc additive manufacture (WAAM) has been conducted for aluminium alloys. In this study, oscillation and parallel deposition strategies were considered for thicker section linear wall building. The results indicate that the deposition strategy has a significant effect on mechanical properties and hardness of the WAAM structure. Optimum ultimate tensile and yield strength were identified after post-deposition heat treatment for both strategies. From microstructure analysis, it was observed that walls produced by oscillation deposition strategy were characterised by equiaxed grains whilst parallel deposited walls were characterised by a mixed grain structure consisting of columnar and equiaxed grains. It was also observed that parallel deposited walls showed an increased number of pores as compared to walls deposited using oscillation strategy. For the studies conducted on aluminium wire + arc additive manufacture, it has been found that the deposition strategy plays an important role in the quality of walls produced.

Keywords: Wire + arc additive manufacture, Cold metal transfer, Aluminium WAAM, Oscillated deposition, Parallel deposition.

1. Introduction

Aluminium alloys have been of high demand to the automobile (Miller et al., 2000) and aerospace (Starke and Staley, 2011) industries to produce parts of improved properties with outstanding light weight to strength ratios. In addition, their good workability and machinability allow different manufacturing techniques to be used by manufacturers to produce complex shapes and patterns (Bai et al., 2016). Wire + arc additive manufacture (WAAM) is attractive due to its ability to produce near net shaped parts and components with high deposition rates coupled with low cost of manufacture. The process incorporates traditional welding techniques such as TIG, MIG and plasma techniques to melt wire layer by layer using computerised numerically controlled gantries or robotic systems (Williams et al., 2015).

Presently, Fronius cold metal transfer process (CMT) has been extensively used in aluminium WAAM for part and component manufacture (Ayarkwa et al., 2015). This process relies on controlled dip transfer mode to produce good quality beads using low heat input with less spatter generation (Pickin et al., 2011). Most research works have been conducted on Al-Cu alloys, specifically AA 2319 and AA 2219 as they are heat treatable and have been used in numerous applications in the aerospace industry. Ayarkwa et al. (2015) investigated the effect of CMT process parameters on AA 2319 linear wall dimensions. Gu et al. (2016a) also conducted studies on the strengthening effect of inter-layer cold working and post-deposition heat treatment of Al-6.3Cu alloy. Cong et al. (2014) studied the effect of CMT arc mode on porosity in linear wall structures. These studies have mainly been conducted on thin linear walls which are limited in wall width during thicker component building. In WAAM, the deposition strategy plays an important role in the manufacture of parts. Therefore for thicker section walls which exceed the limit of single layer wall width, multi-layer deposition strategies have been used. Ding et al. (2015) developed a model for overlapping multi-beads in robotic WAAM. Cong et al. (2017) also compared the effect of CMT arc mode on Al - 6.3%Cu alloy single wall and block structures. The most popular multi-layer deposition strategies are the parallel and oscillation deposition strategies (Bandari et al., 2016). During a parallel deposition, single beads are placed side by side to each other with an overlap, increasing the size of the bead. Therefore, the arc is turned off and on which intend disrupts the deposition after every pass.

On the other hand, in the oscillation strategy, there is no arc disruption prior to the next overlapping weld bead. Figure 1 depicts schematics of both oscillation and parallel multi-layer bead deposition strategies.

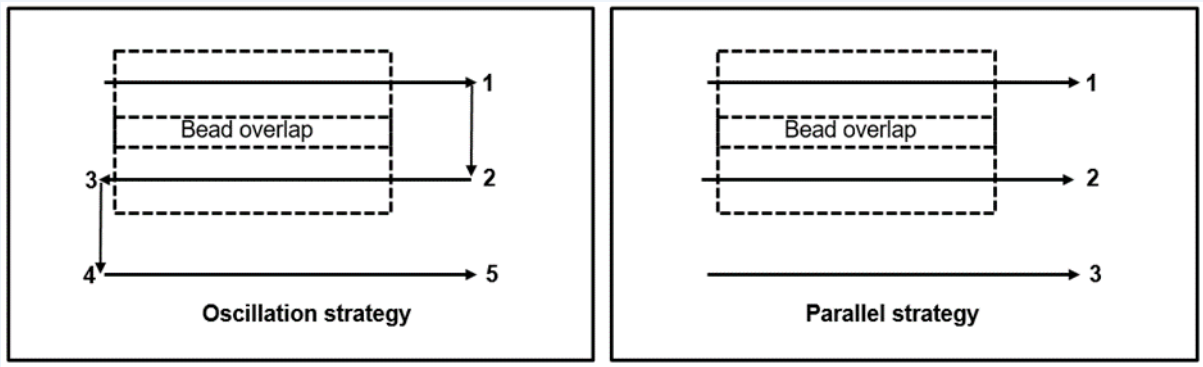

Figure 1: Schematics for oscillation (left) and parallel (right) deposition strategies.

The advantages of the oscillation over parallel strategy include the reduction in fabrication time, process flexibility and high energy efficiency (Bandari et al., 2016). These improve productivity and results from the continuity of the process without disrupting the arc during deposition. Previous studies of different strategies on titanium deposition exhibited different properties (Wang et al., 2019). This is because the deposition strategy has an impact on the thermal cycles which in turn affect the microstructure and mechanical properties differently. However, the effect of the various deposition strategies on wire + arc additive manufacture of aluminium alloys has not been conducted yet.

Therefore, this paper seeks to investigate the effect of parallel and oscillation deposition strategies on aluminium WAAM thicker section linear walls. This will enable the assessment of the effect on mechanical properties, microstructure, and porosity.

2. Experimental setup and procedures

2.1 Materials

In this study, an aluminium 6082-T6 extruded plate of dimension (200 mm x 12.7 mm x 70 mm) was used as the substrate. Aluminium 2319 wire of diameter 1.2 mm was deposited on the substrate. Table 1 shows the material composition of both the wire and the substrate used. Before conducting the experiments, the material substrate was washed in an alkaline solution and then dried. The substrate was then linished mechanically and then finally degreased with acetone prior to deposition.

Material	Composition										
	Al	Si	Mg	Cr	Mn	Ti	Cu	Zn	Fe	Zr	Other
Al 2319	Bal	0.20 Max	0.02 Max	-	0.20-0.40	0.10-0.20	5.8-6.8	0.10-0.25	0.30 max	0.10-0.20	0.15 max
Al 6082-T6	Bal	0.88	0.89	0.06	0.55	0.02	0.08	0.05	0.48	-	0.15

Table 1: Material Composition in wt%

2.2 Equipment set - up

The experimental set – up consisted of an ABB robot (IRB 2400) and the Fronius CMT advance 4000 R power source (Figure 2). The contact tip to work distance was set to 14 mm. Pure shield argon (25 L/min) was used as the shielding gas for creating the inert atmosphere during deposition.

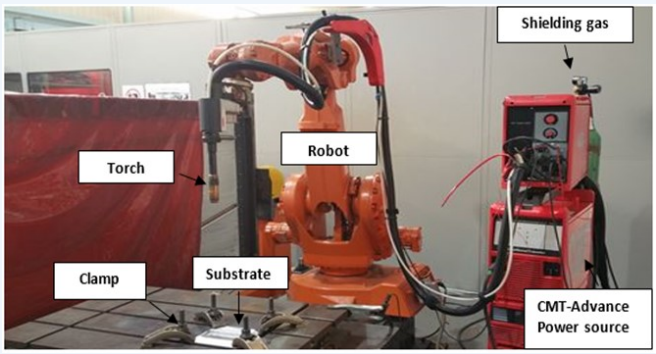

Figure 2: Cold metal transfer WAAM equipment setup

2.3 Experimental and methods

Investigations were carried out using the CMT-pulse (CMT-P) process mode to produce thicker section walls using oscillation and parallel deposition strategies (as shown in Figure 1). The parameters used in performing the experiments are shown in Table 2 where WFS, TS, SBW, LH denote wire feed speed, travel speed, single bead width and layer height, respectively.

Subsequent layers were also deposited on top of the initial layers by using the weld bead height as the layer height increment. Deposited walls were sectioned and grouped into four different conditions. These included oscillated and parallel as-deposited walls and oscillated, and parallel T6 post heat treated walls. For the post heat treatment, a two-stage process was used. This consisted of solution treatment and artificial ageing. Firstly, samples were heated from room temperature to 515 °C at 60 °C/h and then from 515 °C to 535 °C at 20 °C/h. These samples were left at the temperature for 90 min and followed by rapid cooling in cold water. Afterwards, artificial ageing was then conducted at a ramping speed of 60 °C/h from room temperature to 151 °C and then at 20 °C/h from 151 °C to 171 °C for 12 hours. Finally, samples were allowed to cool to room temperature in the furnace.

Process strategy	WFS (m/min)	TS (m/min)	SBW (mm)	LH (mm)	Step advancement (mm)
Oscillation	5	0.6	8.5	2.5	5.6
Parallel	5	0.6	8.5	2.5	5.6

Table 2: Process parameters for oscillated and parallel walls built using CMT-P process

2.4 Microstructure characterisation

Metallographic samples were cold mounted in epoxy. Subsequently, the samples were ground using 240, 600, 1200 and 2500 SiC grit paper. Further polishing was conducted by using 3 µm diamond paste and 1.5 µm colloidal silicon suspension until mirror finish was achieved. Cross section samples were analysed for microstructure, pore distribution and micro hardness. Porosity analysis was conducted 100 mm2 along the deposited walls and analysed using the confocal laser scanning microscope and the IMAGE J software. In this study, the Nikon optihot-66 optical microscope and the scanning electron microscope were used in analysing the microstructure and chemical composition. The hardness measurements were also obtained after applying a load of 200 g at 10 different points using a micro hardness indenter. The average hardness was then calculated after each test.

2.5 Mechanical testing

For mechanical testing, three tensile test specimens were sectioned from the walls in both the longitudinal and transverse directions as depicted by Figure 3a. The sectioned samples were machined to finish as shown in Figure 3b. Tensile tests were then conducted in both the longitudinal and transverse directions using an Instron-5500R in accordance with BS EN ISO 6892 – 1:2009 standard. The capacity of the load cell and test speed used were 30 kN and 1 mm/min respectively

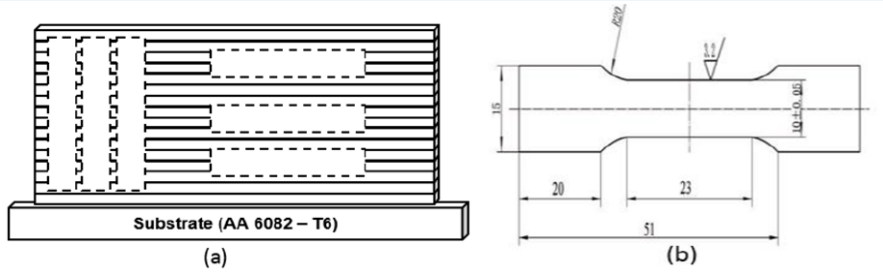

Figure 3: (a) Sectioned directions of tensile specimens and (b) tensile specimen dimensions

3. Results

Figure 4 shows the effect of CMT-P process on thicker section walls for both oscillation and parallel deposition strategies. Both walls are characterised by smut which is the dark substance covering the surface of the walls. The chemical analysis of smut identified in WAAM walls produced was carried out, as shown in Figure 5 and Table 3. The results indicated that darker areas consist of a significant amount of carbon and oxygen as compared to the lighter areas.

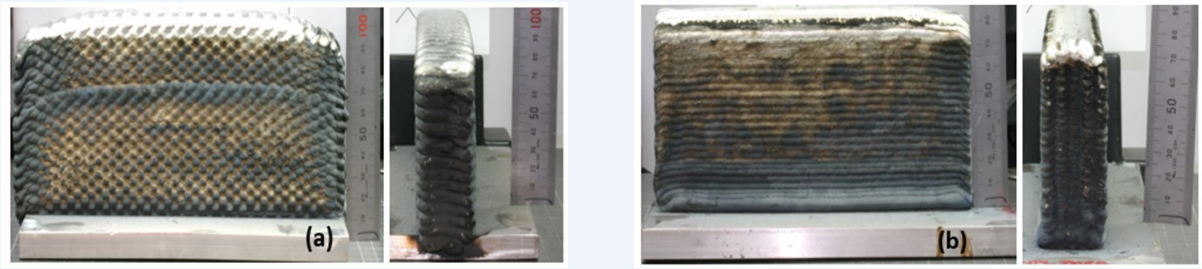

Figure 4: Physical quality of aluminium 2319 WAAM walls produced: (a) oscillated deposited wall; (b) parallel deposited

Citation: Kwasi Frimpong Ayarkwa, et al. "Effect of the deposition strategy on Al-Cu alloy wire + arc additive manufacture". SVR-MSET(1)1 (2021): 28-34.

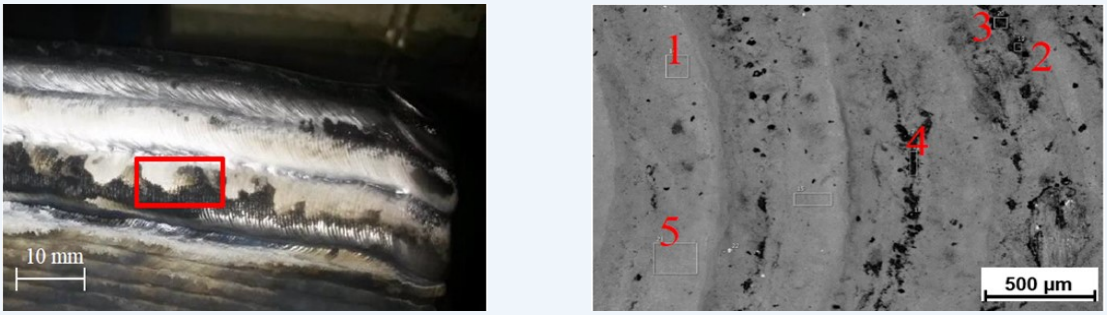

Figure 5: Chemical analysis of smut found on WAAM walls produced

Spectrum Label	C	O	Al	Si	Cu
Spectrum 1	2.06	2.11	90.47	-	5.36
Spectrum 2	40.85	8.28	49.27	0.46	-
Spectrum 3	39.72	15.13	43.55	1.61	-
Spectrum 4	18.27	3.62	74.3	-	3.82
Spectrum 5	1.52	1.97	90.97	-	5.54

Table 3: SEM analysis of Spectrum points

Figure 6 compares the hardness values of oscillated and parallel walls to that of single bead walls in both longitudinal and transverse directions. From the hardness results, oscillated walls display the lowest hardness values in comparison to the other deposition strategies. It was observed that parallel walls and single bead walls exhibited similar hardness values. The results also show no significant variation in the hardness measurement for the different sectioned directions (transverse and longitudinal).

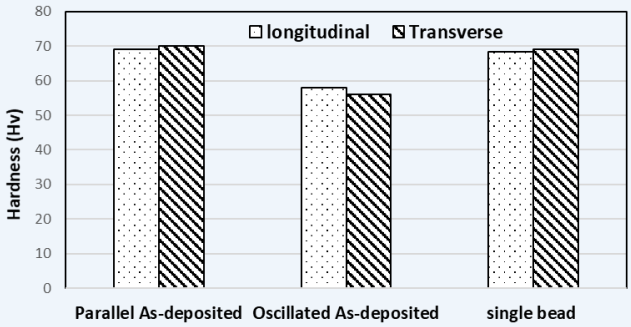

Figure 6: Macro hardness measurement of oscillated, parallel, and single bead as-deposited walls

The optical micrographs of as deposited and post heat treated oscillated and parallel aluminium WAAM walls are shown in Figure 7. In the as-deposited microstructures, the oscillated wall shows equiaxed grains (Figure 7a) whereas parallel wall shows a two-phase structure (Figure 7c) comprising of columnar and refined equiaxed grains. After T6 heat treatment, the grain structures of both strategies were refined with the oscillated wall characterised solely by fine equiaxed grain structure and the parallel wall consisting of columnar and fine equiaxed grains (Figure 7b and d).

From the porosity analysis shown in Figure 8, it can also be seen that both strategies show a substantial number of pores in each area. From pore count analysis, it was identified that the parallel wall displayed a higher pore number and bigger sizes (Figure 8b) as compared to oscillated wall micrograph (8a). It can also be seen that larger pore sizes are mainly at the interphase between layers whereas smaller pores are scattered within the deposit.

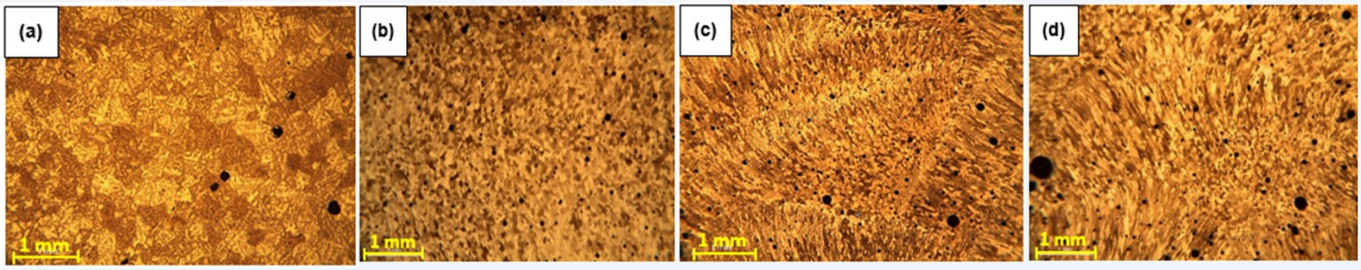

Figure 7: Microstructure of aluminium 2319 WAAM walls: (a) as-deposited oscillated; (b) oscillated post-deposition heat treated T6; (c) as-deposited parallel; (d) parallel post-deposition heat treated T6.

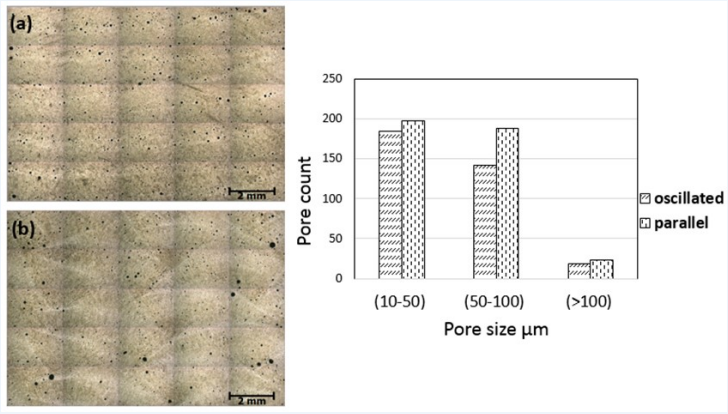

Figure 8: Pore distribution in as-deposited (a) oscillated and (b) parallel walls.

Figure 9 shows the effect of oscillation and parallel deposition strategies on the ultimate tensile strength (UTS), yield strength (YS) and elongation (%) of 2319 aluminium WAAM walls of as deposited and post-deposited T6 heat treated samples. The results show optimum UTS and YS in post-deposited T6 heat treated walls with about 68 % and 50 % increase respectively in comparison to their corresponding as-deposited WAAM walls. It can also be seen that mechanical properties are similar in the different directions of oscillated walls but not for parallel walls. It was observed that elongation in parallel walls were dissimilar for the different test directions for both as deposited and T6 heat treated walls. From the results, maximum elongation was observed in the horizontal direction of parallel as-deposited walls with a corresponding minimum in the vertical direction after T6 treatment. In addition, by comparing mechanical test results of thicker section walls to single bead width walls produced by Gu et al. (Gu et al., 2016a), it can be seen that the UTS and YS results were higher in single bead width walls after T6 treatment with no significant differences in the as-deposited condition. The results also show higher elongation values in the single bead width walls as compared to thicker section walls built.

The fracture surface of WAAM tensile test specimens are shown for the vertical direction of walls produced (Figure 10). It was observed that all tested specimens were characterised by dimples, typical of ductile rupture behaviour. In Figure 10d, the fracture surface is also seen to be characterised by porosity as depicted by the arrow.

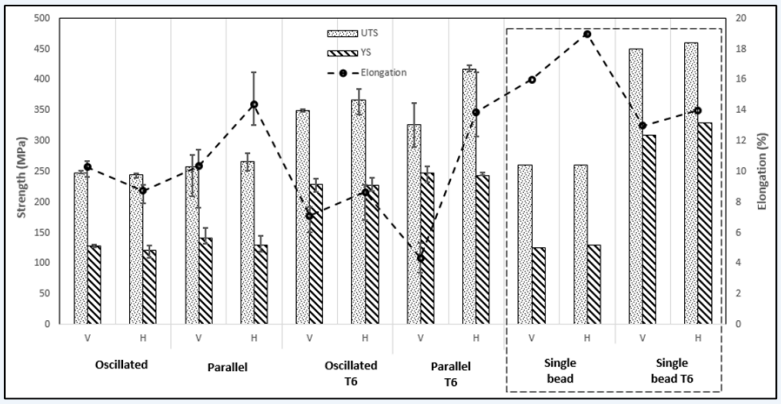

Figure 9: Tensile properties for oscillated and parallel 2319 WAAM walls in comparison to single bead width walls produced by Gu et al. (2016a) in the as-deposited and heat treated conditions (V and H are the vertical and horizontal test directions)

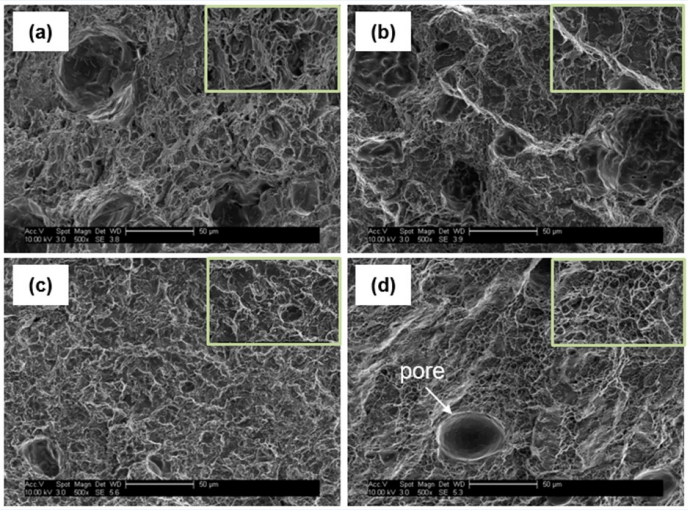

Figure 10: Fracture surface of WAAM 2319 tensile test specimens (a) oscillated as-deposited; (b) oscillated post-deposition T6 heat treated; (c) parallel as-deposited; (d) parallel post-deposition T6 heat treated.

4. Discussion

The capability of CMT-P process has been utilised in thicker section wall building by using parallel and oscillation deposition strategies. In this study, it is evident that walls built by CMT-P process are greatly characterised by smut (Figure 4). Previous studies by Pinter (2017) on aluminium wire + arc additive manufacture highlighted that the quality of the wire could influence the amount of smut formed on the melt bead surface. Ryan et al. (2018) reached the same conclusion using different CMT modes. In this study, the high carbon and oxygen content identified in Table 3 could have resulted from organic contaminants and lubricant residues used in the production process. Additionally, the high heat input of the CMT pulse process could increase the temperature of the melt which in turn causes vaporisation of low boiling point alloy elements such as aluminium, magnesium and zinc to form smut on the surface of melt bead tracks produced (Armao, 2003).

The hardness results show that parallel walls were 20 % greater than oscillated walls built (Figure 6). During parallel deposition, the arc is stopped prior to the deposition of the next overlapping bead, hence the initial bead cools down prior to deposition of subsequent overlapping beads. Therefore, the already cooled melt bead could act as a heat sink to the initial melt bead deposited. The rapid cooling rate of the melt could increase the amount of copper retained in the matrix and this potentially increases the hardness results (Kou, 2003). This can also explain the similar results obtained in the case of single layer bead deposited walls.

From mechanical test results (Figure 9), it is evident that the UTS and YS were maximum after T6 post-deposition heat-treatment. This corroborates studies conducted by Gu et al. (2016b) on the effect of post deposition heat treatment on Al-6.3 Cu single bead deposited linear walls. The authors found that the low strengths of as-deposited walls could be related to their microstructure. These were characterised by the absence of fine strengthening Al2Cu precipitates and segregation of the solute along the grain and dendrite boundaries. Aluminium 2319 is a copper (Cu) based alloy and obtains its strength by precipitation hardening which is affected by time and temperature. During solution treatment, the alloy is heated to a point (between 500 °C and 580 °C) where the second phase (Al2Cu) dissolves in the aluminium matrix (Ashby and Jones, 1998) and then rapidly cooled to retain the Cu in the alloy as metastable supersaturated solid solution. Then fine strengthening precipitates nucleate during the natural or artificial aging (Gu et al., 2016a). Conversely, this may not be the case using the oscillation strategy as there is no arc stop and waiting time. Therefore, a lower temperature gradient may induce coarser second phases which may reduce the strength of the alloy. The difference in elongation values for the different test directions of parallel walls can also be correlated with the microstructure (Figure 7). This consisted of a mixed microstructure of columnar and fine equiaxed grains. Columnar grains are elongated in one direction making the properties different in the different test directions. According to Kurz et al. (2001), columnar growth results from a unidirectional oriented heat flux during heat transfer from a melt into a cooler solid as observed in the case of parallel walls. Conversely, the isotropy of oscillated walls could also be as a result of the coarse equiaxed grain structure resulting from the low temperature gradient of the process. Furthermore, the difference in mechanical properties of T6 heat treated single bead width and thicker section walls of this study could be ascribed to the different aging times used. For this study, longer aging resulted in a reduction in the mechanical properties as compared to work performed on single bead width walls by Gu et al. (2016a). The fracture surface of broken tensile test specimens also depicted ductile fracture for all the walls as observed by the dimples on the surface. Furthermore, the results seemingly indicate that porosity could also be a contributing factor to failure as can be seen in Figure 10d.

The porosity analysis conducted in Figure 8 showed that parallel walls were characterised by increased pore sizes and number as compared to oscillated walls. From studies conducted by Cong et al. (2014), the narrow finger shaped melt pool characteristics of CMT-P process could inhibit the escape of gas pores. Furthermore, the authors also identified a close relationship between porosity and grain size due to the competition between pore nucleation and grain size. This could explain the larger pores identified in parallel walls which are characterised by columnar grains. Moreover, the high cooling rate of parallel walls could result in trapping gas pores as they try to escape prior to solidification. Also, the high amount of smut on the surface of melt bead could also lead to contamination of the melt pool which in turn increases the amount of porosity (Pinter, 2017).

Conclusions

The effect of parallel and oscillation deposition strategies on aluminium wire + arc additive manufacture has been investigated. The following conclusion could be drawn from this research:

- Parallel deposited walls have higher hardness values than oscillated walls.
- The microstructure of parallel deposited walls is characterised by both columnar and equiaxed grains whereas oscillation deposited walls are characterised by equiaxed grains. This can be correlated with the differences in the mechanical properties.
- The ultimate tensile strength and yield strength are maximum with a reduction in elongation after T6 heat treatment.
- Parallel walls displayed increased pore sizes and number as compared to oscillated walls.

Acknowledgement

Kwasi Ayarkwa would like to thank all the WAAMmat program members for supporting his research. The authors would like to thank Armando Caballero, Flemming Nielsen and Steve Pope for their technical support.

References

1. Armao, F., 2003. Aluminum Workshop: How to recognize, minimize weld smut - The Fabricator. Pract. Weld. Today.

2. Ashby, M.F., Jones, D.R.H., 1998. The light alloys, in: Engineering Materials 2. An Introduction to Microstructures, Processing, and Design. Elsevier, Cambridge, UK, pp. 108–121.

Citation: Kwasi Frimpong Ayarkwa, et al. "Effect of the deposition strategy on Al-Cu alloy wire + arc additive manufacture". SVR-MSET(1)1 (2021): 28-34.

3. Ayarkwa, K.F., Williams, S., Ding, J., 2015. Investigation of pulse advance cold metal transfer on aluminium wire arc additive manufacturing. Int. J. Rapid Manuf. 5, 44–57.

4. Bai, L.Y., Lin, S.B., Dong, S.B., Fan, C.L., 2016. Mechanical properties of 2219-Al components produced by additive manufacturing with TIG. Int J Adv Manuf Technol 86, 479–485.

5. Bandari, Y.K., Charrett, T.O.H., Michel, F., Ding, J., Williams, S.W., Tatam, R.P., 2016. Compensation Strategies for Robotic Motion Errors for Additive Manufacturing (AM), in: Proceedings of 27th Annual International Solid Freeform Fabrication Symposium. Texas, USA.

6. Cong, B., Ding, J., Williams, S., 2014. Effect of arc mode in cold metal transfer process on porosity of additively manufactured Al-6.3%Cu alloy. Int. J. Adv. Manuf. Technol. 76, 1593–1606. https://doi.org/10.1007/s00170-014-6346-x.

7. Cong, B., Qi, Z., Qi, B., Sun, H., Zhao, G., Ding, J., 2017. A Comparative Study of Additively Manufactured Thin Wall and Block Structure with Al-6.3%Cu Alloy Using Cold Metal Transfer Process. Appl. Sci. 7, 275. https://doi.org/10.3390/app7030275.

8. Ding, D., Pan, Z., Cuiuri, D., Li, H., 2015. A multi-bead overlapping model for robotic wire and arc additive manufacturing (WAAM). Robot. Comput. Integr. Manuf. 31, 101–110. https://doi.org/10.1016/j.rcim.2014.08.008.

9. Gu, J., Ding, J., Gu, H., Bai, J., Zhai, Y., Ma, P., 2016a. The strengthening effect of inter-layer cold working and post-deposition heat treatment on the additively manufactured Al– 6.3Cu alloy. Mater. Sci. Eng. A 651, 18–26.

10. Gu, J., Ding, J., Williams, S.W., Gu, H., Ma, P., Zhai, Y., 2016b. The effect of inter-layer cold working and post-deposition heat treatment on porosity in additively manufactured aluminum alloys. J. Mater. Process. Technol. 230, 26–34. https://doi.org/10.1016/j.jmatprotec.2015.11.006.

11. Kou, S., 2003. Precipitation-Hardening Materials I: Aluminum Alloys, in: Welding Metallurgy. pp. 353–375. https://doi.org/10.1016/j.theochem.2007.07.017.

12. Kurz, W., Bezençon, C., Gäumann, M., 2001. Columnar to equiaxed transition in solidification processing. Sci. Technol. Adv. Mater. 2, 185–191. https://doi.org/10.1016/S1468-6996(01)00047-X.

13. Miller, W.S., Zhuang, L., Bottema, J., Wittebrood, A.J., De Smet, P., Haszler, A., Vieregge, A., 2000. Recent development in aluminium alloys for the automotive industry. Mater. Sci. Eng. A 280, 37–49. https://doi.org/10.1016/S0921-5093(99)00653-X.

14. Pickin, C.G., Williams, S.W., Lunt, M., 2011. Characterisation of the cold metal transfer (CMT) process and its application for low dilution cladding. J. Mater. Process. Technol. 211, 496–502. https://doi.org/10.1016/j.jmatprotec.2010.11.005.

15. Pinter, Z., 2017. Study of aluminium wire + arc additive manufacture. Cranfield University, UK.

16. Ryan, E.M., Sabin, T.J., Watts, J.F., Whiting, M.J., 2018. The influence of build parameters and wire batch on porosity of wire and arc additive manufactured aluminium alloy 2319. J. Mater. Process. Tech. 262, 577–584. https://doi.org/10.1016/j.jmatprotec.2018.07.030.

17. Starke, E.A., Staley, J.T., 2011. Application of modern aluminium alloys to aircraft, in: Fundamentals of Aluminium Metallurgy: Production, Processing and Applications. Woodhead Publishing Limited, pp. 747–783. https://doi.org/10.1533/9780857090256.3.747.

18. Wang, J., Lin, X., Li, J., Hu, Y., Zhou, Y., Wang, C., Li, Q., Huang, W., 2019. Effects of deposition strategies on macro/microstructure and mechanical properties of wire and arc additive manufactured Ti–6Al–4V. Mater. Sci. Eng. A 754, 735–749. https://doi.org/10.1016/j.msea.2019.03.001.

19. Williams, S.W., Martina, F., Addison, a. C., Ding, J., Pardal, G., Colegrove, P., 2015. Wire+Arc Additive Manufacturing. Mater. Sci. Technol. 32, 641–647. https://doi.org/10.1179/1743284715Y.0000000073.